Dalton Transactions

Accepted Manuscript

Cite this: DOI: 10.1039/c0xx00000x

www.rsc.org/xxxxxx

ARTICLE TYPE

Annealing effects on the properties of $B\mathrm{Fe_2As_2}$ (B = Ca, Sr, Ba) superconducting parents

Bayrammurad Saparov* and Athena S. Sefat

Received (in XXX, XXX) Xth XXXXXXXXX 20XX, Accepted Xth XXXXXXXXX 20XX

DOI: 10.1039/b000000x

The effects of thermal-annealing on the antiferromagnetic (T_N) and structural (T_s) transition temperatures of $ThCr_2Si_2$-type $BaFe_2As_2$ and $SrFe_2As_2$ ('122') crystals are reported, and compared to that of $CaFe_2As_2$. Although the shift in transition temperatures for $CaFe_2As_2$ can be as high as 75 K, we find modest changes of ~ 6 K for $BaFe_2As_2$ and $SrFe_2As_2$. Such findings are based on the measurements of temperature-dependence of electrical resistivity, magnetization, and heat capacity. Residual resistivity ratios show improvement of crystal quality upon anneal for both of $BaFe_2As_2$ and $SrFe_2As_2$. We confirm the pressure-like influence of annealing on 122 crystals.

Introduction

Following the discovery of superconductivity in chemically-doped $BaFe_2As_2$,[1,2] the details of magnetic and structural phase transitions in alkaline-earth based $B\mathrm{Fe_2As_2}$ (B = Ca, Sr, Ba) '122' parents have been the focus of numerous studies.[3-5] At room temperature, the $B\mathrm{Fe_2As_2}$ parents are paramagnetic, and have tetragonal $ThCr_2Si_2$-type structure that features layers of $[FeAs]^-$ made of edge-sharing $FeAs_4$ tetrahedra and B^{2+} layers. These parents exhibit a spin-density-wave (SDW) order of Fe spins below the magnetic ordering temperature (T_N) that is coupled to a low-temperature orthorhombic structural transition (T_s).

The reported values of T_N (T_s) of the 122 parents can be variable depending on the sample preparation conditions,[6-24] presumably, caused by off-stoichiometry or unintentional doping. The use of elemental tin as a flux, for example, results in the incorporation of Sn into the crystals, whereas FeAs self-flux provides crystals free of dopants.[17-22] Interestingly, a recent report indicates that a large ~ 75 K changes in magnetic and structural transition temperatures occur in $CaFe_2As_2$ with post-synthetic annealing treatment.[25] The thermal-annealing, in vacuum or in partial inert atmosphere, are typically aimed at producing chemically-ordered and strain-free crystals. With much surprise however, it was found that annealing can mimic the dramatic effects of applied pressure, causing shifts in transition temperatures by as much as several tens of degrees. This simple high temperature quenching followed by annealing technique allows access of different phases in the temperature (T) – pressure (P) phase diagram for $CaFe_2As_2$, which was previously thought to be accessible only under applied pressure. The $CaFe_2As_2$ samples obtained using this method have distinctly different crystal[26] and electronic[27] structures, and magnetism[26] associated with them. X-ray diffraction and transmission electron microscopy studies show that the as-grown $CaFe_2As_2$ crystals have uniform chemical composition; however, they contain domains with non-uniform strain distribution of lattice parameters. Upon annealing, the strain relief occurs via local and bulk structural changes,[26] which leads a Fermi surface reconstruction[27] and changes in the magnetism of the samples.

Although the large changes in magnetic and structural transition temperatures occurring in $CaFe_2As_2$ are well-documented, a similar experimental study has not been conducted for the $BaFe_2As_2$ and $SrFe_2As_2$. However, there are several reports on the effects of annealing on the properties of $BaFe_2As_2$ and $SrFe_2As_2$. For example, annealing $BaFe_2As_2$ crystal, at 700 °C and for 30 days, shifts T_N = 135 to 140 K, causing sharpened heat capacity anomaly and an order of magnitude decrease of in-plane resistivity (ρ_{ab}).[28] Annealing $SrFe_2As_2$, at 850 °C for 2 days, reduces ρ_{ab} and leads to T_N = 192 K to 200 K,[29] while a short anneal at 300 °C for 5 min is sufficient to remove the strain-induced fractional superconductivity.[30]

Herein, we compare the bulk properties of the as-grown Ba- and Sr- and $CaFe_2As_2$ crystals, and the changes that occur with thermal-annealing. This is a systematic study of annealing effects on Ba122 and Sr122 crystals under the same conditions used for $CaFe_2As_2$ crystals.

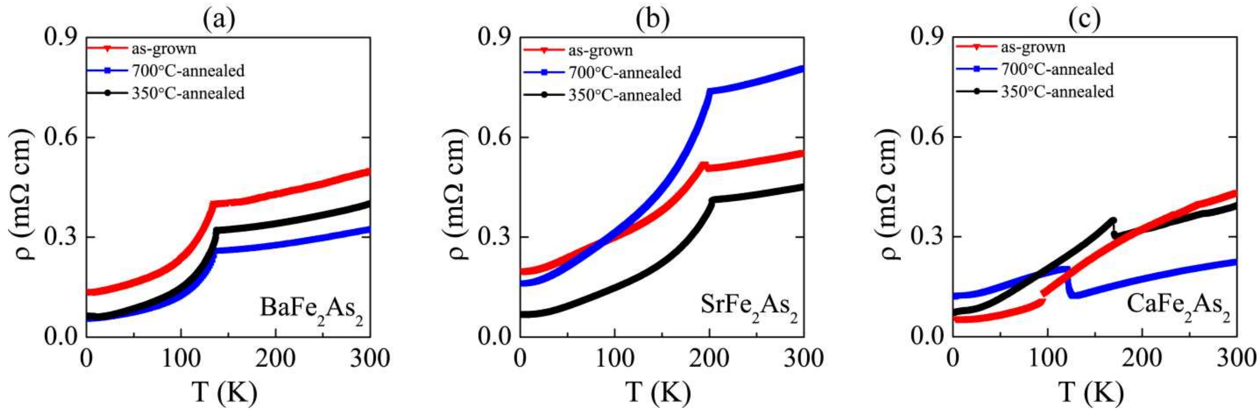

Fig. 1 Resistivity versus temperature for the as-grown and the annealed crystals of (a) $BaFe_2As_2$, (b) $SrFe_2As_2$, and (c) $CaFe_2As_2$ measured upon warming in the *ab* plane.

Table 1 Transition temperatures (T^*) determined from $d\rho/dT$, $d(\chi T)/dT$), and $C(T)$ data, for the as-grown and annealed BFe_2As_2 (B = Ca, Sr, Ba) crystals. Dashed-line indicates 'not measured'

History	$d\rho/dT$		Fisher's $d(\chi T)/dT$)	$C(T)$
	on cooling	*on warming*	*on warming*	*on cooling*
$BaFe_2As_2$				
as-grown	134(1) K	134(1) K	129(2) K	132(1) K
700°C-annealed (1 d)	135(1) K	135(1) K	135(1) K	-
700°C-annealed (30 d)	135(1) K	136(1) K	137(1) K	137(1) K
350°C-annealed (5 d)	137(1) K	138(1) K	138(1) K	-
$SrFe_2As_2$				
as-grown	195(1) K	196(1) K	197(2) K	-
700°C-annealed (1 d)	199(2) K	200(1) K	197(3) K	-
350°C-annealed (5 d)	201(1) K	202(1) K	203(1) K	-
$CaFe_2As_2$				
as-grown	90(1) K	95(1) K	96(1) K	92(1) K
700°C-annealed (1 d)	118(2) K	122(1) K	118(4) K	111(1) K
350°C-annealed (5 d)	168(1) K	170(1) K	171(1) K	168(2) K

Results and discussions

Electrical resistivity and magnetization

Temperature dependence of electrical resistivity, $\rho(T)$, for BFe_2As_2 (B= Ca, Sr, Ba) crystals are presented in Fig. 1. All materials display metallic behavior with ρ decreasing upon cooling. There are discontinuities, labelled as T^*, in ρ in all of the BFe_2As_2 crystals. There is an inverse dependence for ΔT^* with size of alkaline-earth metal, with ionic size $Ca^{2+} < Sr^{2+} < Ba^{2+}$.[31] The largest ΔT^* is observed for $CaFe_2As_2$, with as-grown crystal giving T^* = 95(1) K and 350°C-annealed crystal with T^* = 170(1) K (Fig. 1c), whereas for $SrFe_2As_2$ and $BaFe_2As_2$, ΔT^* from resistivity data are ~ 6 K and 4 K, respectively. In all cases, 350°C-annealed crystals give the highest T^*, while the as-grown crystals give the lowest T^* values; 700°C-annealed crystals give T^* values that lie in between that for as-grown and 350°C-annealed crystals. There is a small hysteresis at T^* in $\rho(T)$ measured on warming and cooling, with the largest hysteresis of ~ 5 K seen for the as-grown $CaFe_2As_2$ crystal. The complete list of changes in transition temperatures for all of these materials are listed in Table 1.

Increase in residual resistivity ratio (RRR = $\rho_{300\ K}/\rho_{2\ K}$) with annealing corroborates with the trend in transition temperatures from resistivity data for $BaFe_2As_2$ and $SrFe_2As_2$; RRR values rise from 3.6 for as-quenched to 6.3 for 350 °C-annealed crystals of $BaFe_2As_2$, and from 2.8 to 6.7 for $SrFe_2As_2$. Such a trend is expected assuming that crystal quality increases with annealing. Indeed, it has been reported that annealing $BaFe_2As_2$ crystals together with BaAs at 800 °C for 5 days results in a 10-fold increase of RRR,[32] while annealing under partial argon gas pressures at 700°C for 30 days leads to a 7-fold rise.[28] In contrast to these reports, our results indicate only a modest ~ 2-fold increase of RRR for $SrFe_2As_2$ and $BaFe_2As_2$. However, for $CaFe_2As_2$, the RRR values decrease with annealing: they are 8.0 for as-grown, 5.4 for 350°C-annealed and 1.9 for 700°C-annealed crystals. Such a markedly differing trend can be tied to the magnetic, local and bulk structural changes in $CaFe_2As_2$, which occur with annealing as we have found recently.[26]

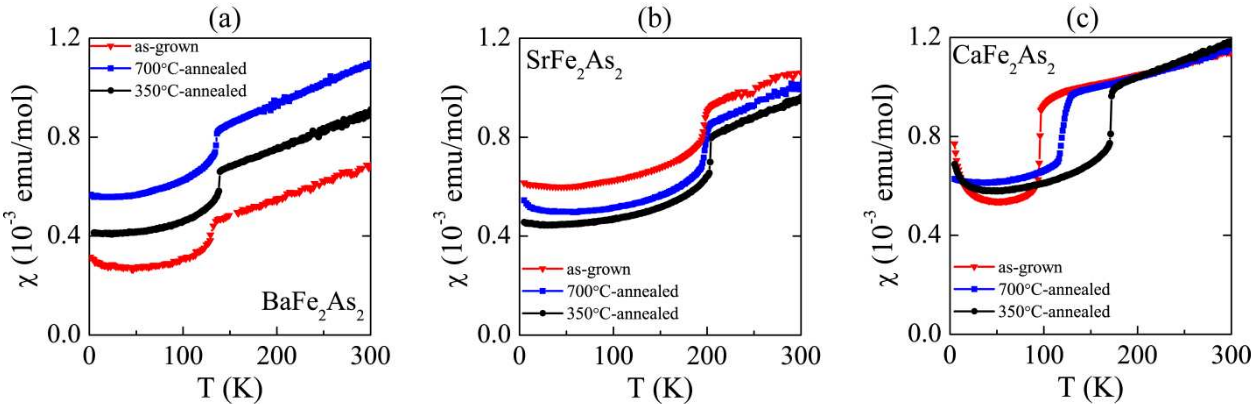

Fig. 2 Temperature dependence of magnetic susceptibility, χ(T), in the applied field of 1 Tesla in the *ab*-plane for (a) $BaFe_2As_2$, (b) $SrFe_2As_2$, and (c) $CaFe_2As_2$.

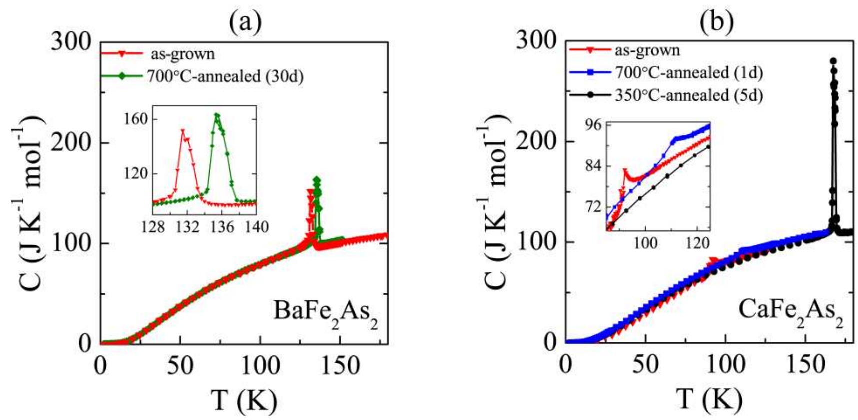

Fig. 3 Heat capacity versus temperature, $C(T)$, for as-grown and an annealed crystals of (a) $BaFe_2As_2$ and (b) $CaFe_2As_2$.

ZFC temperature-dependent magnetic susceptibility data, $\chi(T)$, are presented in Fig. 2. There is a sharp downturn at T^* in $\chi(T)$ plots of BFe_2As_2, above which there is a linear increase. The transition temperature T^* values extracted from Fisher's $d(\chi T)/dT$ analysis (see Table 1) are comparable to those found in $d\rho/dT$.

Heat capacity

Temperature dependence of heat capacity results for $CaFe_2As_2$ and $BaFe_2As_2$ are plotted Fig. 3, and summarized in Table 1. For the as-grown $BaFe_2As_2$ crystal, the Sommerfeld coefficient is $\gamma \approx$ 6 mJ/(mol K^2), which compares well with 6.1 mJ/(mol K^2) value reported in literature.[28,33] For the prolonged 700 °C-annealed $BaFe_2As_2$ crystal, we surprisingly find no significant change with γ = 6.4 mJ/(mol K^2). Earlier reports suggest sharpening of $C(T)$ peak and ~ 5 K increase in T^* after 700 °C-anneal for 30 days,[28] however, we only find identical peak widths and a similar 5 K increase in T^*. In comparison, for $CaFe_2As_2$, there is a noticeable decrease in the γ values with $\gamma \approx$ 14 mJ/(mol K^2) for the as-grown, $\approx$ 6 mJ/(mol K^2) for 350 °C-annealed, and $\approx$ 8 mJ/(mol K^2) for 700 °C-annealed crystals.[26] From the strong peaks in the heat capacity data, it is evident that the magnetic and structural transitions coincide for the as-grown and annealed crystals of Ba122, and the 350 °C-annealed crystal of Ca122. We have recently found[26] that the broad peak in the 700 °C-annealed Ca122 crystal is due to the gradual transition over 40 K range, whereas only a structural transition occurs over 5 K range in the as-grown crystal.

A significant expansion of the *c*-parameter has been reported for $CaFe_2As_2$ upon annealing at 350 ºC, as evidenced by a more than 1° (2θ) shift in the (0 0 8) peak positions in the PXRD patterns.[26] The *c*-parameter increases from c = 11.574(1) Å in the as-grown crystal to c = 11.7262(8) Å in the 350 ºC-annealed $CaFe_2As_2$ crystal at room temperature. The *c*-parameter is the gauge of pressure in BFe_2As_2, and in the case of $CaFe_2As_2$, compression of the *c*-parameter leads to disappearance of the hole cylinders and the Fermi surface nesting, resulting in a nonmagnetic collapsed tetragonal phase. However, the (0 0 8) peak shifts for $SrFe_2As_2$ and $BaFe_2As_2$ are less than 0.05°, suggesting very small changes in the *c*-parameters (below 0.01 Å). Consequently, this implies that the Fermi surface modification is small in $SrFe_2As_2$ and $BaFe_2As_2$, consistent with only small changes in antiferromagnetic transition temperatures upon annealing.

Conclusions

The dramatic changes in the structural (T_s) and magnetic (T_N) transitions temperatures occurring in the quenched crystals of $CaFe_2As_2$ with annealing have been likened to the effect of the pressure.[25,26] Indeed, earlier studies have shown that polycrystalline $CaFe_2As_2$ is extremely pressure sensitive, and as little as 1.7 GPa at 300 K is sufficient to induce a structural collapse from the high temperature tetragonal to the collapsed tetragonal phase.[34] Owing to the larger sizes of Sr^{2+} and Ba^{2+} cations,[31] $SrFe_2As_2$ and $BaFe_2As_2$ have much higher critical pressure values of P_c = 10 GPa (nonhydrostatic conditions)[35] and P_c = 27 GPa,[34] respectively. Based on these, the effects of annealing on the quenched crystals of $SrFe_2As_2$ and $BaFe_2As_2$ are expected to be much less significant. In agreement with this conjuncture, our experimental results on the as-grown and annealed crystals of $SrFe_2As_2$ and $BaFe_2As_2$ show that the shifts in the transition temperature are 5 K and 6 K, respectively. Additionally, the structural parameters that influence the transition temperatures do not show significant changes with annealing. The changes in the *c*-parameters for $SrFe_2As_2$ and $BaFe_2As_2$, for example, are less than 0.01 Å. Annealing leads to improved crystal qualities as evidenced by the increase in RRR values from 2.8 to 6.7 for $SrFe_2As_2$, and from 3.6 to 6.3 for $BaFe_2As_2$. This is in contrast with the lowering of RRR values in $CaFe_2As_2$ from 8 down to 1.9 with annealing. The difference in the trends in RRR is likely due to the remarkable changes in the structure and magnetism of $CaFe_2As_2$.

Temperature dependence of heat capacity experiments display modest changes for the as-grown and the 700 °C-annealed crystals of $BaFe_2As_2$. The peak widths do not change with annealing, in contrast to the earlier reports,[28] the peaks at transition temperatures are very strong for both crystals. The sharp peaks in the heat capacity data indicate that the magnetic and structural transitions coincide for the as-grown and annealed crystals of $BaFe_2As_2$, similar to the 350 °C-annealed crystal of $CaFe_2As_2$.

In conclusion, this work confirms the expected pressure-like effects of annealing on $SrFe_2As_2$ and $BaFe_2As_2$. In the next step, the structural and magnetic changes in BFe_2As_2 could be explored through variation of the quenching temperatures, *i.e.* temperatures where FeAs-flux is removed via centrifugation, in addition to the ongoing doping studies.

Experimental

BFe_2As_2 (B = Ca, Sr, Ba) single crystals were grown out of FeAs flux by the reaction of elemental alkaline-earth metals with FeAs binary. Reaction mixtures were heated to 1190°C, kept at this temperature for 24 hours, and then slowly cooled to 960°C for B = Ca, 990°C for B = Sr, and 1090°C for B = Ba, at which point the FeAs flux was decanted by spinning each reaction in a centrifuge. These spin temperatures were taken from literature; the resulting plate-like crystals are called 'as-grown,' following the nomenclature used for them in literature. From each reaction batch, several crystals of BFe_2As_2 were selected for heat treatment studies; temperatures of annealing were chosen at350°C and 700 °C, similar to those in literature.[25,26]

Energy-dispersive X-ray spectroscopy (EDS) was performed using a Hitachi-TM3000 scanning electron microscope equipped with a Bruker Quantax 70 EDS system. Scanning over ~ 100 μm × 100 μm area of the crystals, the results confirmed 1:2:2 elemental compositions for as-grown, and also for the annealed crystals of BFe_2As_2.Temperature-dependence of electrical resistivity$\rho_{ab}(T)$ and heat capacity $C(T)$ measurements on BFe_2As_2 crystals were performed on a Quantum Design Physical Property Measurement System. Electronic (γ) and lattice (β) contributions to the heat capacity were extracted from the linear fits of C/T vs T^2 plots below 10 K. Temperature-dependence of magnetization experiments were carried out using a Quantum Design Magnetic Property Measurement System. Applied fields of 10 kOe along the *ab*-plane were used to collect zero-field-cooled (ZFC) magnetization data. Estimations of transition temperatures (T*) were done by dρ/dT and Fisher's $d(\chi T)/dT$. Powder X-ray Diffraction (PXRD) measurements were carried out on a PANalytical X'Pert PRO MPD with monochromated Cu-Kα_1 radiation. The flat-lying BFe_2As_2 crystals were used to collect (0 0 *l*) Bragg peaks, and subsequently, to estimate the *c*-lattice parameters from their Le Bail fits.

Acknowledgments

This work was supported by the Department of Energy, Basic Energy Sciences, Materials Sciences and Engineering Division.

Notes and references

Materials Science & Technology Division, Oak Ridge National Laboratory, P. O. Box 2008, Building 4100, 1 Bethel Valley Road, Oak Ridge, TN 37831-6056, USA. Fax:8655765023; Tel: 8655764747; E-mail: saparovbi@ornl.gov

1 M. Rotter, M. Tegel and D. Johrendt, *Phys. Rev. Lett.*, 2008, **101**, 107006.
2 A. S. Sefat, R. Y. Jin, M. A. McGuire, B. C. Sales, D. J. Singh and D. Mandrus, *Phys. Rev. Lett.*, 2008, **101**, 117004.
3 Q. Huang, Y. Qiu, W. Bao, M. A. Green, J. W. Lynn, Y. C. Gasparovic, T. Wu, G. Wu and X. H. Chen, *Phys. Rev. Lett.*, 2008, **101**, 257003.
4 A. Jesche, N. Caroca-Canales, H. Rosner, H. Borrmann, A. Ormeci, D. Kasinathan, H. H. Klauss, H. Luetkens, R. Khasanov, A. Amato, A. Hoser, K. Kaneko, C. Krellner and C. Geibel, *Phys. Rev. B*, 2008, **78**, 180504.
5 A. I. Goldman, D. N. Argyriou, B. Ouladdiaf, T. Chatterji, A. Kreyssig, S. Nandi, N. Ni, S. L. Bud'ko, P. C. Canfield and R. J. McQueeney, *Phys. Rev. B*, 2008, **78**, 100506.
6 G. Wu, H. Chen, T. Wu, Y. L. Xie, Y. J. Yan, R. H. Liu, X. F. Wang, J. J. Ying and X. H. Chen, *J. Phys.: Condens. Matter*, 2008, **20**, 422201.
7 F. Ronning, T. Klimczuk, E. D. Bauer, H. Volz and J. D. Thompson, *J. Phys.: Condens. Matter*, 2008, **20**, 322201.
8 N. Kumar, R. Nagalakshmi, R. Kulkarni, P. L. Paulose, A. K. Nigam, S. K. Dhar and A. Thamizhavel, *Phys. Rev. B*, 2009, **79**, 012504.
9 P. C. Canfield, S. L. Bud'ko, N. Ni, A. Kreyssig, A. I. Goldman, R. J. McQueeney, M. S. Torikachvili, D. N. Argyriou, G. Luke and W. Yu, *Physica C*, 2009, **469**, 404.
10 P. M. Shirage, K. Miyazawa, H. Kito and A. Iyo, *Appl. Phys. Express*, 2008, **1**, 81702.
11 J. Zhao, W. Ratcliff II, J. W. Lynn, G. F. Chen, J. L. Luo, N. L. Wang, J. Hu and P. Dai, *Phys. Rev. B*, 2008, **78**, 140504.
12 H. Li, W. Tian, J. L. Zarestky, A. Kreyssig, N. Ni, S. L. Bud'ko, P. C. Canfield, A. I. Goldman, R. J. McQueeney and D. Vaknin, *Phys. Rev. B*, 2009, **80**, 054407.
13 S. R. Saha, N. P. Butch, K. Kirshenbaum and J. Pagloine, *Phys. Rev. B*, 2009, **79**, 224519.
14 J. Q .Yan, A. Kreyssig, S. Nandi, N. Ni, S. L. Bud'ko, A. Kracher, R. J. McQueeney, R. W. McCallum, T. A. Lograsso, A. I. Goldman and P. C. Canfield, *Phys. Rev. B*, 2008, **78**, 024516.
15 C. Krellner, N. Caroca-Canales, A. Jesche, H. Rosner, A. Ormeci and C. Geibel, *Phys. Rev. B*, 2008, **78**, 100504.

16 K. Kaneko, A. Hoser, N. Caroca-Canales, A. Jesche, C. Krellner, O. Stockert and C. Geibel, *Phys. Rev. B*, 2008, **78**, 212502.
17 M. Rotter, M. Tegel, D. Johrendt, I. Schellenberg, W. Hermes and R. Pottgen, *Phys. Rev. B*, 2008, **78**, 020503.
18 X. F. Wang, T. Wu, G. Wu, H. Chen, Y. L. Xie, J. J. Ying, Y. J. Yan, R. H. Liu and X. H. Chen, *Phys. Rev. Lett.*, 2009, **102**, 117005.
19 J. K. Dong, L. Ding, H. Wang, X. F. Wang, T. Wu, G. Wu, X. H. Chen and S. Y. Li, *New J. Physics*, 2008, **10**, 123031.
20 A. S. Sefat, R. Jin, M. A. McGuire, B. C. Sales, D. Mandrus, F. Ronning, E. D. Bauer and Y. Mozharivskyj, *Phys. Rev. B*, 2009, **79**, 094508.
21 N. Ni, S. L. Bud'ko, A. Kreyssig, S. Nandi, G. E. Rustan, A. I. Goldman, S. Gupta, J. D. Corbett, A. Kracher and P. C. Canfield, *Phys. Rev B*, 2008, **78**, 014507.
22 Y. Su, P. Link, A. Schneidewind, T. Wolf, P. Adelmann, Y. Xiao, M. Meven, R. Mittal, M. Rotter, D. Jonhrendt, T. Brueckel and M. Loewenhaupt, *Phys. Rev. B*, 2009, **79**, 064504.
23 Z. Ren, Z. W. Zhu, S. A. Jiang, X. F. Xu, Q. Tao, C. Wang, C. M. Feng, G. H. Cao and Z. A. Xu, *Phys. Rev. B*, 2008, **78**, 052501.
24 H. S. Jeevan, Z. Hossain, D. Kasinathan, H. Rosner, C. Geibel and P. Gegenwart, *Phys. Rev. B*, 2008, **78**, 052502.
25 S. Ran, S. L. Bud'ko, D. K. Pratt, A. Kreyssig, M. G. Kim, M. J. Kramer, D. H. Ryan, W. N. Rowan-Weetalutuk, Y. Furukawa, B. Roy, A. I. Goldman and P. C. Canfield, *Phys. Rev. B*, 2011, **83**, 144517.
26 B. Saparov, C. Cantoni, M. Pan, T. C. Hogan, W. Ratcliff II, S. D. Wilson, K. Fritsch, B. D. Gaulin and A. S. Sefat, *Sci. Rep.*, 2014, **4**, 4120.
27 K. Gofryk, B. Saparov, T. Durakiewicz, A. Chikina, S. Danzenbächer, D. V. Vyalikh, M. J. Graf and A. S. Sefat, http://arxiv.org/abs/1404.1095.
28 C. R. Rotundu, B. Freelon, T. R. Forrest, S. D. Wilson, P. N. Valdivia, G. Pinuellas, A. Kim, J.-W. Kim, Z. Islam, E. Bourret-Courchesne, N. E. Phillips and R. J. Birgeneau, *Phys. Rev. B*, 2010, **82**, 144525.
29 J. Gillett, S. D. Das, P. Syers, A. K. T. Ming, J. I. Espeso, C. M. Petrone and S. E. Sebastian, http://arxiv.org/abs/1005.1330v1.
30 S. R. Saha, N. P. Butch, K. Kirshenbaum and J. Paglione, *Physica C*, 2010, **470**, S379.
31 R. D. Shannon, *Acta Crystallogr.*, 1976, **A32**, 751.
32 M. Nakajima, T. Liang, S. Ishida, Y. Tomioka, K. Kihou, C. H. Lee, A. Iyo, H. Eisaki, T. Kakeshita, T. Ito and S. Uchida, *Proc. Natl. Acad. Sci.*, 2011, **108**, 12238.
33 J. K. Dong, L. Ding, H. Wang, X. F. Wang, T. Wu, G. Wu, X. H. Chen and S. Y. Li, *New J. Phys.*, 2008, **10**, 123031.
34 R. Mittal, S. K. Mishra, S. L. Chaplot, S. V. Ovsyannikov, E. Greenberg, D. M. Trots, L. Dubrovinsky, Y. Su, Th. Brueckel, S. Matsuishi, H. Hosono and G. Garbarino, *Phys. Rev. B*, 2011, **83**, 054503.
35 W. O. Uhoya, J. M. Montgomery, G. M. Tsoi, Y. K. Vohra, M. A. McGuire, A. S. Sefat, B. C. Sales and S. T. Weir, *J. Phys.: Condens. Matter*, 2011, **23**, 122201.

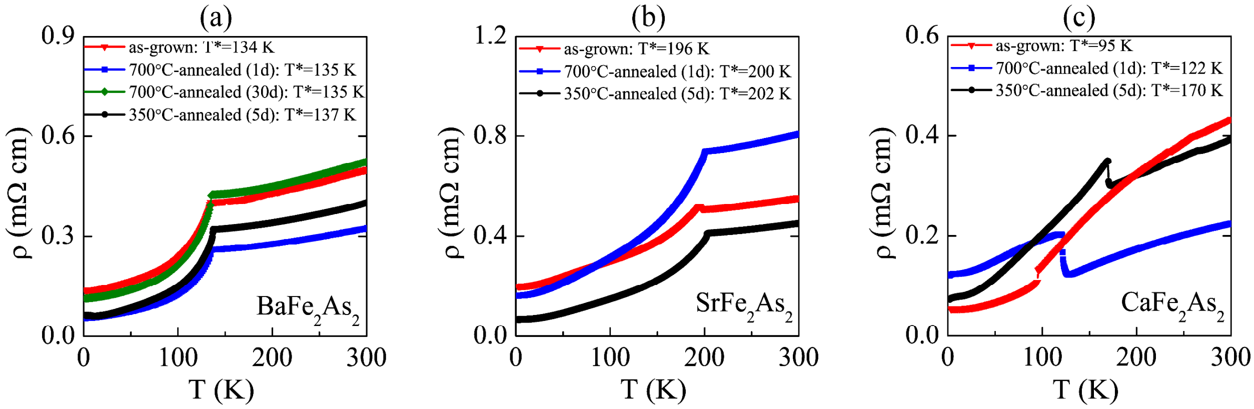

Thermal annealing and results in ~ 6 K shift in the structural and magnetic transition temperatures of $BaFe_2As_2$ and $SrFe_2As_2$.